A Solar Plasma Stream Measured by DRVID and Dual-Frequency Range and Doppler Radio Metric Data

F. B. Winn and S. C. Wu
Tracking Systems and Applications Section

T. A. Komarek
Telecommunications Systems Section

V. W. Lam, H. N. Royden, and K. B. W. Yip
Navigation Systems Section

S- and X-band DRVID, S- and X-band dual-frequency range (SX (ρ)), and doppler (SX ($\dot{\rho}$)) measured a 15-fold increase in the line-of-sight electron content of the solar plasma above the normal plasma background. A general increase in the plasma electron content continued for nearly 50 hours: it started about 12:00 (GMT) on 12 March 1976 and continued to grow until 17:00 (GMT) on 14 March. For the next 55 hours, between 17:00 (GMT) on 14 March to 00:54 (GMT) on 17 March, the plasma level diminished as the background level was again approached.

Not only were the temporal changes and absolute level of the plasma content measured but the measurements were also used to ascertain the mean-plasma-concentration location: it was estimated to be 4.1 light minutes from Earth.

It is demonstrated that if round-trip S-band range is to be calibrated for plasma influence to the meter level, then some knowledge of the plasma distribution must exist.

I. Introduction

Two Viking spacecraft were navigated to Mars by analyzing radio metric data acquired from the spacecraft while they were in heliocentric orbits. When the spacecraft were at a geocentric distance of ~1.2 AU and were angularly 96 deg from the Sun as viewed from Earth, S- and X-band DRVID, S- and X-band dual-frequency range (SX (ρ)) and doppler (SX ($\dot{\rho}$)) measured a 15-fold increase in the line-of-sight electron content of the solar plasma above the normal plasma background. A general increase in the plasma electron content continued for nearly 50 hours: it started about 12:00 (GMT) on 12 March 1976

and continued to grow until 17:00 (GMT) on 14 March. For the next 55 hours, between 17:00 (GMT) on 14 March to 00:54 (GMT) on 17 March, the plasma level diminished as the background level was again approached.

Not only were the temporal changes and absolute level of the plasma content measured but the measurements were also used to ascertain the mean-plasma-concentration location: it was estimated to be 4.1 light minutes from Earth.

An examination of the radio metric data in the presence of this plasma shows:

(1) S-band group delays as large as 27 m occurred (3.33 ns/m).

(2) S-band phase changed at rates up to 3.6 m/h.

(3) S-band doppler rms noise was at 14 mHz at one time (~6 times greater than nominal for 60-second count time doppler).

(4) S-band doppler rms noise does not necessarily correlate with plasma level.

II. Charged-Particle Calibrations

Electromagnetic group and phase velocities are slowed down and speeded up, respectively, by electron concentrations as shown by

$$V_g = c\left(1 - \frac{1}{2}\frac{Ne^2}{4\pi^2\epsilon_0 mf^2}\right)$$

$$V_p = c\left(1 + \frac{1}{2}\frac{Ne^2}{4\pi^2\epsilon_0 mf^2}\right)$$

where

V_g = group velocity (modulation)

V_p = phase velocity (carrier)

c = velocity of light (2.998×10^8 m/s)

e = electron charge (-1.602×10^{-19} coulombs)

ϵ_0 = free space permittivity (8.85×10^{-12} farad/m)

m = electron mass (9.109×10^{-31} kg)

f = carrier frequency (Hz)

N = density of electrons along propagation path (electrons/m^3)

The transit time for modulation propagating at the group velocity between the spacecraft ($x = 0$) and station ($x = R$) is

$$T_g = \int_0^R \frac{dx}{V_g}$$

Similarly, the transit time for the carrier phase is

$$T_p = \int_0^R \frac{dx}{V_p}$$

Using the formula for V_g and V_p, and introducing the integrated electron content $I = \int N dx$, gives the group and phase transit times between the spacecraft and Earth-bound station:

$$T_g = \frac{R}{c} + \frac{1}{2}\frac{e^2}{4\pi^2\epsilon_0 mf^2} I$$

$$T_p = \frac{R}{c} - \frac{1}{2}\frac{e^2}{4\pi^2\epsilon_0 mf^2} I$$

where

T_g = group transit time

T_p = phase transit time

R = distance between spacecraft and station (m)

$I = \int_0^R N dx$ = integrated electron content along signal path (electrons/m^2)

The charged-particle calibration data types (Table 1) exploit the dispersive nature of the plasma or the opposite, but equal, influence of the plasma on group and phase velocities.

III. Plasma Event as Measured

Prior to March 1976, when the Sun-Earth-probe (SEP) angle was >96 deg, very little plasma activity was apparent (Fig. 1). Figure 1 shows the amount of phase shifts due to changes in columnar content experienced by S-band radio waves. Each plotted point shows the accumulated phase shifts over a view period. Since the view periods were of variable time duration, many of the lower points can be ignored. The connected line segments (which tie together tracking passes greater than 6 hours in duration) offer a coarse estimate of the relative plasma activity from November 1975 to March 1976. The peak-to-peak phase shifts over each view period were divided by the time interval in hours to give the average hourly rates (Fig. 2). These also reveal the two large plasma events in the month of March. These plasma events are detected when plasma concentrations cross the Earth-spacecraft propagation paths, which move almost perpendicular to the solar radial (Fig. 3).

The absolute plasma content, as measured by SX (ρ), shows the 15 March plasma event to have commenced to cross the Viking raypaths at about 15:00 (GMT) on 12 March (Fig. 4). The plasma concentration continued to move onto the raypaths until ~55 hours later on 17 March. Relative plasma levels, as indicated by S-band differenced range versus integrated doppler (DRVID) and SX ($\dot{\rho}$), are consistent with SX (ρ) (Fig. 4).

SX (ρ) absolute content calibrations are negatively biased. SX (ρ) and Faraday rotation (Ref. 3) calibrations of the electron content of Earth's ionosphere appear to have a 6-m offset (Fig. 5). The SX (ρ) calibration is approximately 6 m less than the Faraday calibration independent of DSS (Table 2) or Viking spacecraft. This SX (ρ) was acquired from Viking 1975 (VK '75) spacecraft A when the probe was 146 deg from the Sun as seen from Earth and at a distance of ~0.3 AU. Thus, the probability is high that the plasma contribution to SX (ρ) is small ($\ll$1 m). This negative 6-m bias has been corrected for in Fig. 4.

The total electron content (Fig. 4) at 12:00 (GMT) on 12 March results in an S-band range delay of 5.5 m. At 16:52 (GMT) on 12 March, the combined electron content equals $\sim 16 \times 10^{17}$ electrons/m^2, which produces an S-band range delay of ~20.5 m. At this time, the ionospheric content is $\sim 10^{17}$ electrons/m^2, and the plasma content is $\sim 15 \times 10^{17}$ electrons/m^2. The plasma level changes 11.5×10^{17} electrons/m^2 in 4 hours 52 minutes. Following this rise in content at a rate of 2.3×10^{17} electrons/m^2/hour for ~5 hours, a less rapid, linear accumulation of $\sim 0.2 \times 10^{17}$ electrons/m^2/hour was observed for about the next 45 hours. It reached a maximum level of $\sim 20 \times 10^{17}$ electrons/m^2 (27 m of S-band range delay) at 16:32 (GMT) on 14 March. This maximum level persisted for at least 9 hours. At 01:00 (GMT) on 15 March, the data were interrupted for ~13 hours. When the SX ($\dot{\rho}$) calibrations were once again acquired at ~13:00 (GMT) on 15 March, the electron content was at $\sim 14 \times 10^{17}$ electrons/m^2 (19 m of S-band range delay). SX ($\dot{\rho}$), SX (ρ), and S-band DRVID are consistent and show another ~9-m decrease in the S-band range delay between 13:00 (GMT) on 15 March and 02:00 (GMT) on 16 March. Subsequent data passes continued to reveal a general decrease in the plasma level. It was not until 19 March that SX (ρ) calibrations were again at the ionospheric content level.

IV. Plasma Stream Influence on S-Band Doppler

Root-mean-square S-band doppler noise increased 5- to 6-fold as the plasma stream swept through the line-of-sight (Fig. 6). This increase in noise stems from the high frequency fluctuations of the plasma (plasma turbulence, Ref. 4), which scintillates radio carriers. S-band doppler is acquired from the Viking probes nearly continuously. A running 2-hour average of the doppler noise (Fig. 7) compares the noise levels of the Viking 1 and 2 spacecraft doppler. The angular separation of the 2 probes is 1.1 deg. The maximum linear separation of the probe line-of-sight is ~0.02 AU. Since large-scale plasma structures usually extend over distances of tenths of AU or more, it is expected that the rms noise levels of the radio carriers will correlate highly as shown in Fig. 7. If the total doppler scintillation is directly proportional to the total electron content of the plasma at large SEP angles (i.e., 96 deg) as indicated by researchers (Refs. 4 and 5) for small SEP angles (i.e., <5 deg), then the rms noise pattern suggests two peaks in the line-of-sight electron content. One peak occurs between 06:00 and 14:00 (GMT) on 14 March and the second between 02:00 and 16:00 (GMT) on 15 March. On 14 March when SX (ρ) is indicating a maximum plasma electron content of 20×10^{17} electrons/m^2, S-band doppler rms noise is at its lowest level. This suggests that at large SEP angles the net scintillation of a radio carrier is not necessarily directly proportional to the line-of-sight electron content. Additional investigation is needed.

V. Plasma Mean Distance Estimate

Transmissions to the spacecraft are at S-band frequencies; transmissions from the spacecraft are at S- and X-band frequencies. S-band DRVID is a round-trip measurement; SX ($\dot{\rho}$) is downleg only in character.

If the space plasma concentration is (1) singular, (2) localized, and (3) fixed in space, then a DRVID-SX ($\dot{\rho}$)

cross-correlation yields the mean distance of the plasma concentration from the spacecraft. The procedure is to find that Δt for which the minimum rms difference between DRVID and 2-way SX ($\dot{\rho}$) exists:

$$\text{minimum} \sum_t \{\text{DRVID}_t - [\text{SX}(\dot{\rho})_t + \text{SX}(\dot{\rho})_{t-\Delta t}]\}^2$$

for Δt = 1,2,3, . . . , round-trip light minutes from plasma to probe to plasma.

If the plasma concentration is at the spacecraft, then the light-time separation between upleg and downleg encounters with the plasma is zero ($\Delta t = 0$).

The rms difference for $\Delta t = 0$ is then

$$\sum_t [\text{DRVID}_t - 2\,SX(\dot{\rho})_t]^2$$

Fig. 8 shows 2 SX ($\dot{\rho}$) and DRVID for the 15 March view period. The rms difference equals 0.4 m, which is 2 times the DRVID rms noise.

If the plasma were located at Earth, then the separation in time between plasma encounters would equal the total round-trip time from Earth to spacecraft to Earth. For the plasma concentration assumed at Earth (Fig. 9), the rms discrepancy between DRVID and $[\text{SX}(\dot{\rho})_t + \text{SX}(\dot{\rho})_{t-18.2}]$ is 0.7 m.

For an 11-minute light-time separation between upleg and downleg encounters, a minimum rms difference of 0.2 m is obtained (Fig. 10). Thus, $[\text{SX}(\dot{\rho})_t + \text{SX}(\dot{\rho})_{t-11}]$ and DRVID calibrations are in closest agreement when the concentration is assumed 4.1 light minutes from Earth (5.5 minutes from the spacecraft) and are shown in Fig. 11.

Once the light-time separation between plasma encounters, Δt, is known, SX (ρ) and SX ($\dot{\rho}$) yield round-trip range calibrations for plasma dynamics. First, SX ($\dot{\rho}$) is fit to SX (ρ) such that a minimum rms difference results (Fig. 12). For the 15 March data, a minimum rms difference of 0.3 m is obtained for the two SX measurement types. Now SX ($\dot{\rho}$), as plotted, possesses absolute plasma level information. The round-trip range calibration is then:

$$\text{SX}(\dot{\rho})_t + \text{SX}(\dot{\rho})_{t-\Delta t}$$

If a comparison is made between 2 SX $(\dot{\rho})_t$ and SX $(\dot{\rho})_t$ + SX $(\dot{\rho})_{t-\Delta t}$ at each point within the pass, the maximum difference is ~0.3 m. This is comparable to the rms uncertainty of the SX (ρ) - SX ($\dot{\rho}$) fit. Thus, in this case, computing the "true" upleg calibration did not make much difference: however, as the SEP angle diminishes (plasma levels increase) and as the spacecraft-to-Earth light-time increases (more time separation between upleg and downleg plasma encounters), it is expected that plasma influences on upleg and downleg doppler and range will become increasingly different. For example, for the 15 March plasma (Fig. 12), if the spacecraft to plasma light-time distance was ½ hour, then the doubled downleg SX $(\rho)_t$ minus $[\text{SX}(\dot{\rho})_t + \text{SX}(\dot{\rho})_{t-\Delta t}]$ difference is >3 m at the point where SX ($\dot{\rho}$) has its greatest slope.

The Mariner Jupiter-Saturn mission will place the spacecraft ~10 AU from Earth (round-trip light-time ~160 minutes). Round-trip S-band range acquired by multiple DSS, when differenced, is required to a $4.5\sqrt{2}$-m accuracy (1σ). That is the total error due to all error sources. To realize this accuracy, differenced range calibrations for plasma effects must be achieved to at least the meter level.

If the time interval between range measurements is small (10-20 minutes), then it appears that much of the plasma effects in the two range measurements will cancel in the difference. To what extent cancellation occurs is currently under study.

VI. Summary

S- and X-band DRVID, S- and X-band dual-frequency range, and doppler have been used to determine the absolute and relative electron content of a plasma concentration. The plasma appears to have taken more than 100 hours to cross the radio propagation paths between Earth and the Viking space probes. At times the electron content was ~20 X 10^{17} electrons/m^2.

The mean location of the plasma concentration was determined from 15 March 1976 data to be 4.1 minutes away from Earth.

The Sun-Earth-probe angle was ~96 deg.

It is demonstrated that if round-trip S-band range is to be calibrated for plasma influence to the meter level, then some knowledge of the plasma distribution must exist.

References

1. MacDoran, P. F., "A First-Principles Derivation of the Differenced Range Versus Integrated Doppler (DRVID) Charged-Particle Calibration Method," in *The Deep Space Network,* Space Programs Summary 37-62, Vol. II, pp. 28-34, Jet Propulsion Laboratory, Pasadena, Calif., Mar. 31, 1970.

2. Madrid, G. A., "The Measurement of Dispersive Effects Using the Mariner 10 S- and X-Band Spacecraft to Station Link," in *The Deep Space Network Progress Report 42-22,* pp. 22-27, Jet Propulsion Laboratory, Pasadena, Calif., Aug. 15, 1974.

3. Yip, K. W., et al., "Decimeter Modeling of Ionospheric Columnar Electron Content at S-Band Frequencies," edited by J. M. Goodman, *Symposium on Effect of the Ionosphere on Space Systems and Communications, Naval Research Laboratory, Washington, D. C., Jan. 20-22, 1975,* p. 345.

4. Anderson, J. D., et al., "A Measurement of the General Relativistic Time Delay with Data from Mariner 6 and 7," edited by R. W. Davies, *Proceedings of the Conference on Experimental Tests of Gravitation Theories, California Institute of Technology, Pasadena, Calif., Nov. 11-13, 1976,* p. 111.

5. Berman, A. L., and Wackley, J. A., "Doppler Noise Considered as a Function of the Signal Path Integration of Electron Density," in *The Deep Space Network Progress Report 42-33,* pp. 159-193, Jet Propulsion Laboratory, Pasadena, Calif., June 15, 1976.

Table 1. Charged-particle calibration data types[a]

Type/principle	Formulation
DRVID (differenced range versus integrated doppler) exploits the opposite, but equal, effect of the electron content on group and phase velocities (Ref. 1).	$\text{DRVID} = \frac{c}{2}\{\rho_s(t_i) - \rho_s(t_0) - K[\Phi_s(t_i) - \Phi_s(t_0) - f_b(t_i - t_0)]\}$ DRVID = S-band phase shift, m; t_0 = reference time c = velocity of light, m/s; f_b = frequency bias, Hz ρ_s = S-band round-trip travel time, s; K = constant, s/cycle Φ_s = S-band phase, cycles; t_i = observation time
SX ($\dot{\rho}$) (dual-frequency dispersive doppler) exploits the inverse squared relationship between phase change and carrier frequency in an electron medium (Ref. 2).	$\text{SX}(\dot{\rho}) = \Phi_s - \frac{3}{11}\Phi_x$ Φ_x = X-band phase, cycles
SX (ρ) (dual-frequency dispersive range) also exploits the inverse frequency squared dependence of group velocity in an electron medium (Ref. 2).	$\text{SX}(\rho) = \rho_s(t_i) - \rho_x(t_i)$ (group delay) $\rho_x(t_i)$ = X-band group travel time, s

[a]In a companion article, "Solar Plasma: Viking 1975 Interplanetary Spacecraft Dual-Frequency Doppler Data," a summary of the plasma history throughout the heliocentric, ballistic "cruise" phase of the Viking mission is provided. Additionally, some comparisons of the calibrations derived from DRVID, dispersive doppler are offered.

Table 2. Deep Space Station coordinates

DSS	Location	λ, deg	Distance from Earth spin-axis, km
14	Goldstone, California	243.11047	5203.999
43	Canberra, Australia	148.98127	5205.252
63	Robledo, Spain	355.75198	4860.819

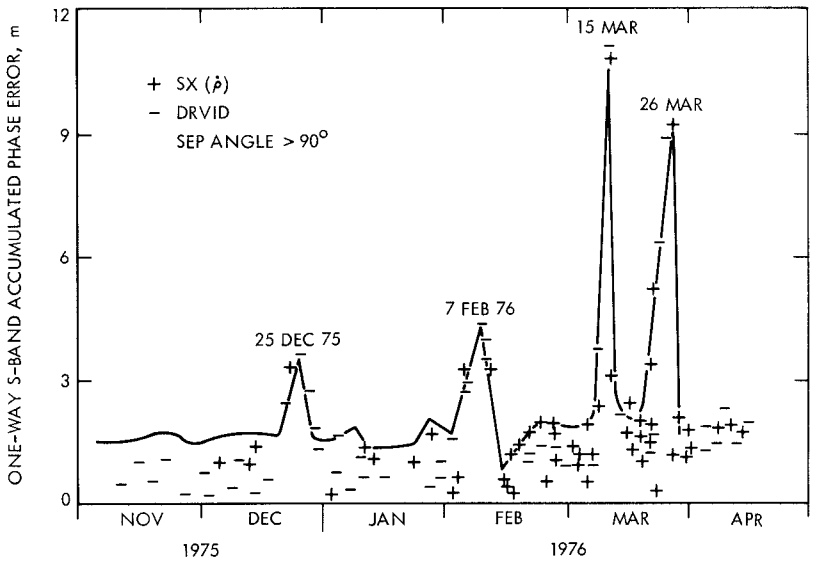

Fig. 1. Viking A observed plasma dynamics

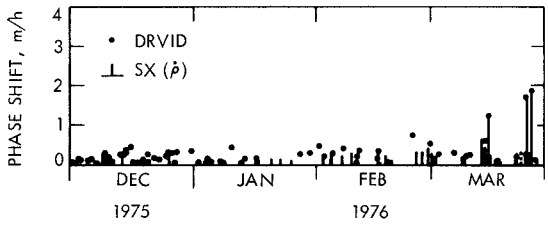

Fig. 2. Viking A average phase shift per hour

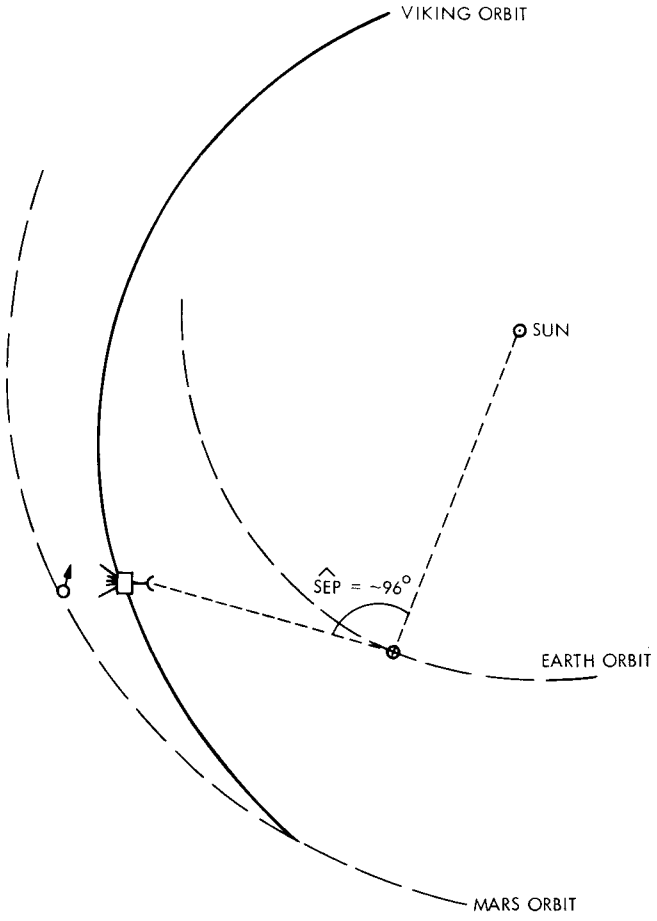

Fig. 3. Angular separation of Viking spacecraft from Sun as viewed from Earth

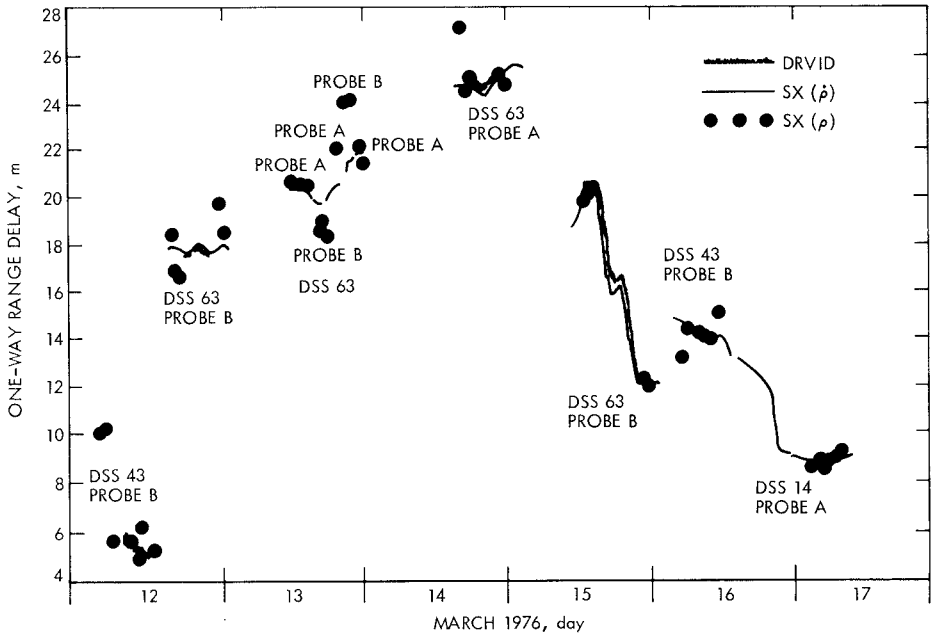

Fig. 4. SX (ρ), SX ($\dot{\rho}$), S-band DRVID measurements of solar plasma plus Earth's ionosphere

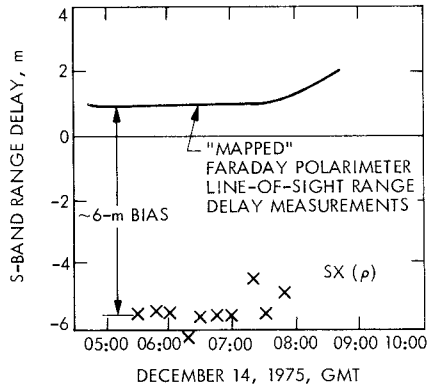

Fig. 5. Comparison of ionospheric measurements with SX (ρ)

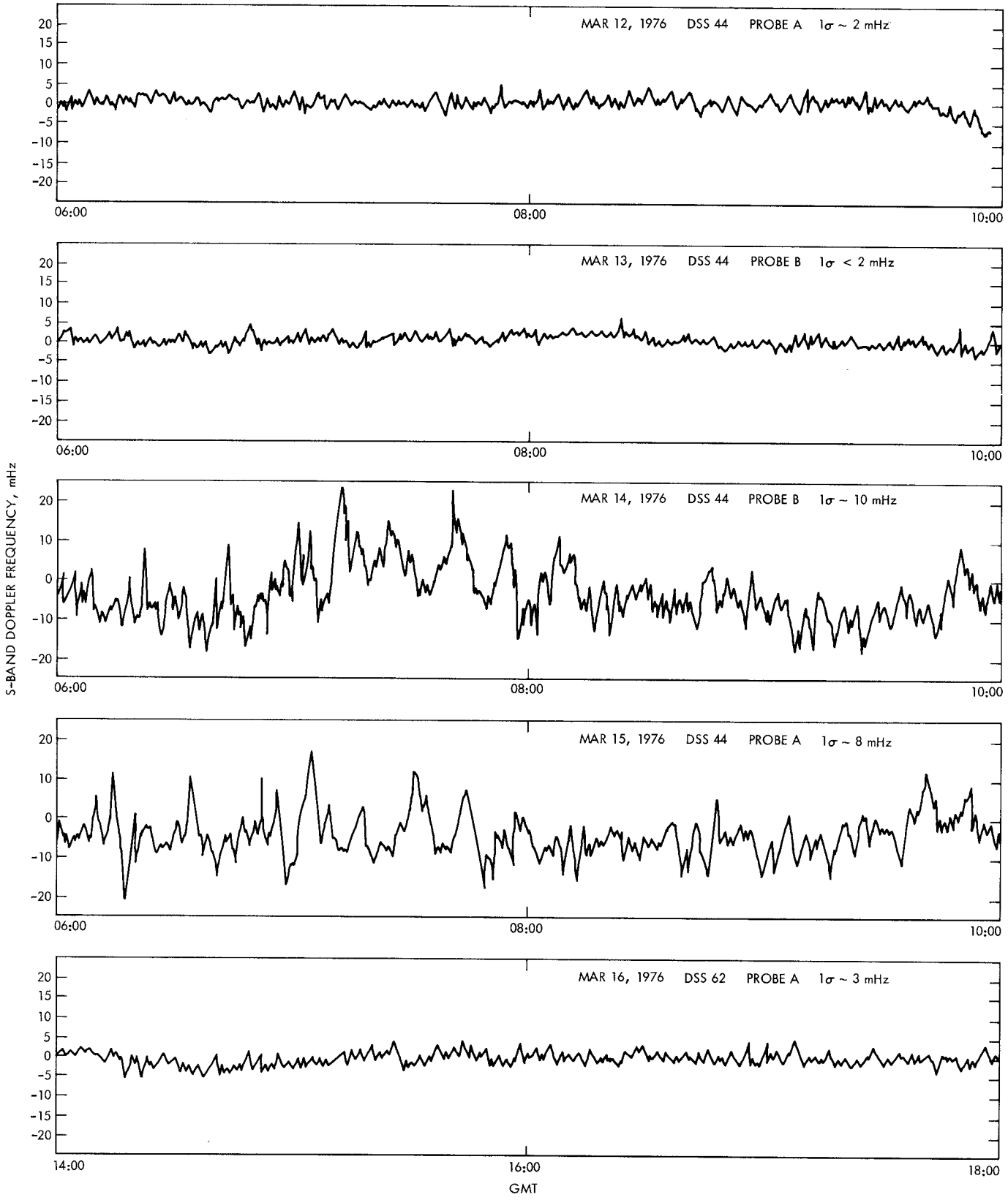

Fig. 6. Doppler noise characteristics as a function of plasma activity

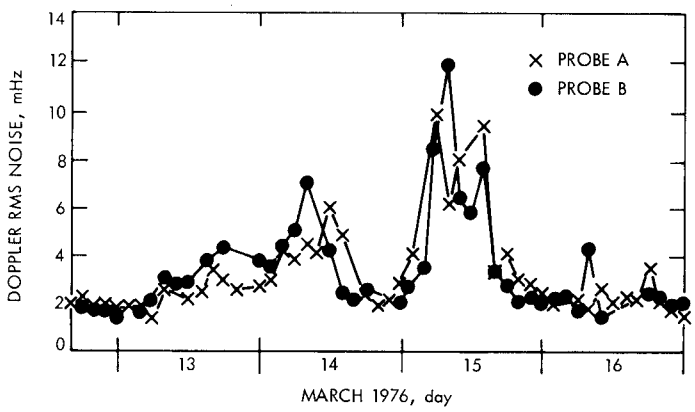

Fig. 7. Rms doppler noise during plasma disturbance

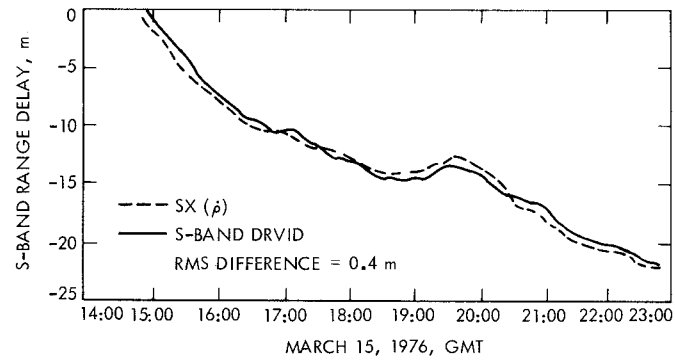

Fig. 8. Round-trip 2-way effects with plasma concentration assumed at spacecraft

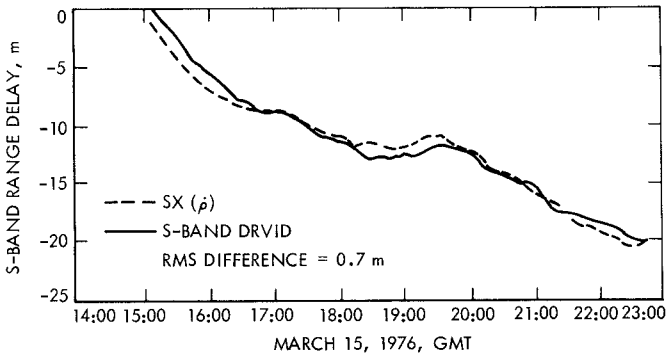

Fig. 9. Round-trip 2-way effects with plasma concentration assumed at Earth

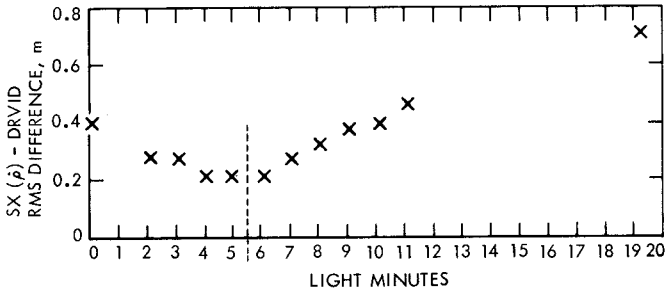

Fig. 10. Estimated light-time separation between upleg and downleg plasma encounters

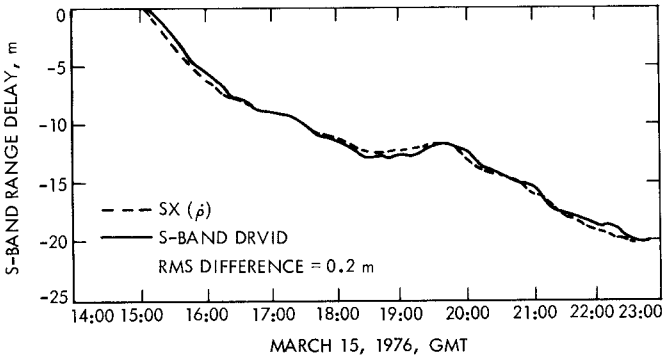

Fig. 11. Round-trip 2-way effects with plasma concentration assumed at 4.1 light minutes from Earth

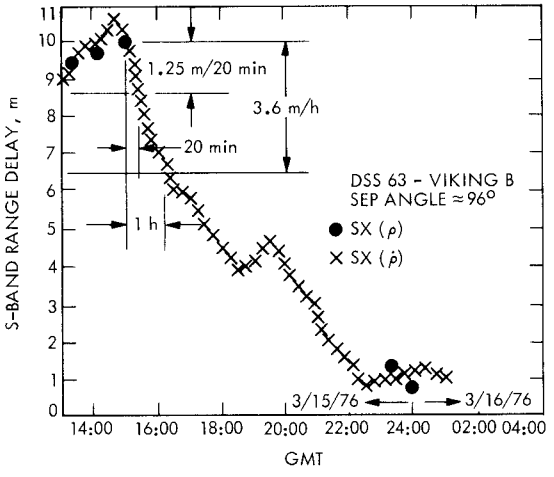

Fig. 12. Upleg/downleg range delay differences for 20-minute and 1-hour light-time separations between upleg/ downleg plasma encounters